JOURNAL OF AIRCRAFT
Vol. 44, No. 6, November–December 2007

Analysis of Visual Cues During Landing Phase by Using Neural Network Modeling

Ryota Mori* and Shinji Suzuki†
University of Tokyo, Tokyo 113-8656, Japan
Yuki Sakamoto‡
All Nippon Airways, Tokyo 144-8515, Japan
and
Hiroshi Takahara§
All Nippon Airways, Osaka 563-0034, Japan

DOI: 10.2514/1.30208

A neural network modeling approach has been developed to analyze the pilot's use of visual cues for landing a transport airplane. Time sequences of the visual cues and pilot control inputs obtained by using a flight simulator can be analyzed to quantitatively estimate the relationship between the visual cues and the pilot control inputs. In this paper, visual cues such as the horizon, runway shape, and runway marker are compared based on their importance. By using a flight simulator, neural network models are obtained in all cases wherein a pilot intentionally alters his or her attentiveness to the visual cues. The contribution ratios analysis reflects the attentiveness to each visual cue. The Monte Carlo landing simulation shows the difference in robustness of each obtained neural network model. It is confirmed that the timely choice of the appropriate visual cue is necessary for a smooth and safe landing.

I. Introduction

VISUAL cues are primarily used for guidance and control information during human operations. Experienced pilots use visual cues properly according to the circumstances; therefore an analysis of the role of each visual cue is important to improve the skill of the pilots and the design of display systems. Because it is difficult to analyze human operations quantitatively and logically, the use of mathematical models of human operations and the application of optimal control theory to analyze the effect of visual cues on the performance index have been reported in the literature [1–3]. However it is difficult to construct accurate human operation models because each pilot possesses unique characteristics that can be adapted according to the situation.

Recently neural network (NN) modeling has been recognized as a powerful technique to simulate and analyze human operations [4]. The authors have presented an NN model of a pilot's landing maneuvers by using flight data obtained from a flight simulator [5]. Artificial NNs are mathematical models that emulate the biological nervous system; they consist of a large number of highly interconnected processing elements such as neurons [6]. The parameters of the NN model are adjusted by a learning process. Although neuron has a simple transfer function, NNs can relate input/output data that have high nonlinearity.

Although pilots use several visual cues such as instrument displays or actual out-the-window views, they do not have sufficient time to read the instrument data during the final landing phase and must estimate airspeed, descent rate, altitude, and pitch angle of the plane by using visual cues through the cockpit windows. The skill of the pilot in this estimation is important for a smooth landing [7]. The authors have applied NNs to analyze airplane pilots' maneuvers during the landing phase [5]. The input data for the NNs are the visual cues, for example, runway geometry and the horizon, as well as the previous control column input. The output data from the NNs are the current control column and throttle lever deflections. In the previous study, a clear distinction was found between the use of visual cues by a freshman pilot and that by a veteran pilot. In this paper, we analyze the importance of visual cues such as the horizon, runway shape, and runway marker by using NN models. The NN models are obtained in all cases wherein a pilot intentionally changes his or her attentiveness to the visual cues by using a flight simulator.

This paper is organized as follows. In Sec. II, the application of genetic algorithms (GAs) to optimize the generalization capability of the NN model is briefly summarized. In Sec. III, the influence of each visual cue on the pilot control input during a landing task is investigated. First the contribution of each visual cue is evaluated for the different flight data obtained by using a PC-based flight simulator for a midsize jet airliner when a pilot intentionally concentrates on a specified visual cue. Second the obtained NN models are used as automatic controllers for Monte Carlo flight simulations where the initial flight conditions fluctuate randomly. The Monte Carlo flight simulations are employed to evaluate the role of each visual cue. The conclusions are provided in Sec. IV.

II. Neural Network Modeling with Genetic Algorithms

An artificial NN is applied to the mathematical modeling of human maneuvers. An artificial neuron is a simple processing element, as shown in Fig. 1. Mathematically, the operation of the neuron can be represented as follows:

$$y = f\left(\sum_{i=1}^{n}(w_i x_i + b/n)\right) \tag{1}$$

where x_i and w_i represent the input and weight, respectively, and b is the threshold or bias of the activation function f.

A network created by the combination of a few simple artificial neurons can exhibit complex behavior. A three-layer network is used in this study, as shown in Fig. 2. Here, the system has n inputs and l outputs, and the activation function in each layer is defined as

Presented as Paper 6498 at the AIAA Atmospheric Flight Mechanics Conference and Exhibit, Keystone, CO, 21–24 August 2006; received 2 February 2007; revision received 23 April 2007; accepted for publication 25 April 2007.

*Graduate Student, Department of Aeronautics and Astronautics, 7-3-1 Hongo, Bunkyo-ku.
†Professor, Department of Aeronautics and Astronautics, 7-3-1 Hongo, Bunkyo-ku; tshinji@mail.ecc.u-tokyo.ac.jp. Senior Member AIAA.
‡Flight Operations–Engineering, Haneda Airport 3-3-2, Ota-ku.
§767 Captain, Deputy Director, Osaka Flight Crew Center B767 Pilot Office, Osaka International Airport 2-1-10, Kuko, Ikeda-shi.

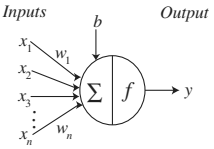

Fig. 1 Basic neuron model.

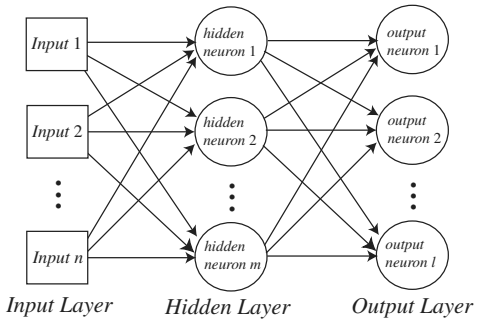

Fig. 2 Neural network model.

follows:

$$f:\begin{cases} x\mapsto 1/(1+e^{-x}) & \text{(hidden layers)} \\ x\mapsto x & \text{(output layers)} \end{cases} \tag{2}$$

Therefore the output of the network is generated as follows:

$$y_j^h = f\left[\sum_{i=1}^{n}\left(w_{j,i}^h x_i + b_j^h/n\right)\right] \tag{3}$$

$$y_k^o = \sum_{j=1}^{m}\left(w_{k,j}^o y_j^h + b_k^o/m\right) \tag{4}$$

where the super indexes h and o represent the hidden and output layers, respectively. In our study, the contribution and contribution ratio of the input x_i $(i = 1, \ldots, n)$ to the output y_k $(k = 1, \ldots, l)$ are calculated in the following manner to analyze the information flows in the network [4]:

$$C_{k,i} = \sum_{j=1}^{m}\left|w_{j,k}^h x_i + b_j^h/n\right|\cdot\left|w_{k,j}^o y_j^h + b_k^o/m\right| \tag{5}$$

$$R_{k,i} = \frac{\sum_{j=1}^{m}\left|w_{j,k}^h x_i + b_j^h/n\right|\cdot\left|w_{k,j}^o y_j^h + b_k^o/m\right|}{\sum_{i=1}^{n}\sum_{j=1}^{m}\left|w_{j,k}^h x_i + b_j^h/n\right|\cdot\left|w_{k,j}^o y_j^h + b_k^o/m\right|} \tag{6}$$

Although the contribution ratio does not indicate the accurate percentage of contribution for each parameter, a qualitative analysis can still be discussed.

The learning process of the network is carried out to minimize the mean square error between the teaching output data set and the corresponding computed output data set. The weights $\boldsymbol{w}$ and biases $\boldsymbol{b}$ of the neurons are obtained by the learning process by using the error back-propagation method.

When NN models are created for complex problems, the generalization capability of the model must be confirmed. Generalization refers to the ability of the NN to produce reasonable outputs for inputs that are not encountered during training. The network structure and the global optimality of solutions have an influence on the generalization capability of the obtained NN. The authors have proposed the use of GAs to optimize the number of neurons in the hidden layer and the initial values of the weights and biases of the network. An increase in the number of hidden layer neurons can provide a precise fitting performance for the network; however the network may become highly sensitive to measurement noise. Because there are no specific guidelines for the selection of the number of hidden layer neurons, a trial-and-error approach is usually used. On the other hand, although the weights and biases of the network are computed using the back-propagation method, it is important to select appropriate initial values to obtain the global optimal solution for complicated problems. A GA uses search procedures based on the mechanics of natural genetics, which uses a Darwinian survival-of-the-fittest strategy to eliminate the unfit characteristics and random information exchange [8]. Because it can simultaneously handle integers and real variables and is generally recognized as being able to find the global optimal solution, the GA approach is introduced to select both the number of hidden layer neurons and the initial values of the optimization parameters, that is, the weights and the biases in the network.

The generalization capability of the obtained NN is examined for a test data set $\boldsymbol{t}^*$ that is slightly different from the teaching data. The cost function to be minimized in the GA is the weighted sum of the mean square error (MSE) for the teaching data set and the MSE for the test data set, as expressed below.

$$F_{\mathrm{GA}}(\boldsymbol{w}_{\mathrm{ini}}, \boldsymbol{b}_{\mathrm{ini}}, n_{\mathrm{hid}}) = E[(\boldsymbol{t}-\boldsymbol{a})^T(\boldsymbol{t}-\boldsymbol{a})] + \alpha E[(\boldsymbol{t}^*-\boldsymbol{a}^*)^T(\boldsymbol{t}^*-\boldsymbol{a}^*)] \tag{7}$$

where $\boldsymbol{w}_{\mathrm{ini}}$, $\boldsymbol{b}_{\mathrm{ini}}$, and n_{hid} are the initial values of the weights, biases, and the number of hidden layers to be optimized in the GA, respectively. Note that $\boldsymbol{a}^*$ is the output data set computed from the network when provided with the input data set $\boldsymbol{t}^*$, and α is a scaling factor. Figure 3 illustrates the GA optimization of the NN. $\boldsymbol{w}_{\mathrm{ini}}$, $\boldsymbol{b}_{\mathrm{ini}}$, and n_{hid} are coded into a discrete binary string called a gene. It fully specifies a potential solution. An initial population of potential solutions is created by assigning. A cost function of each gene is

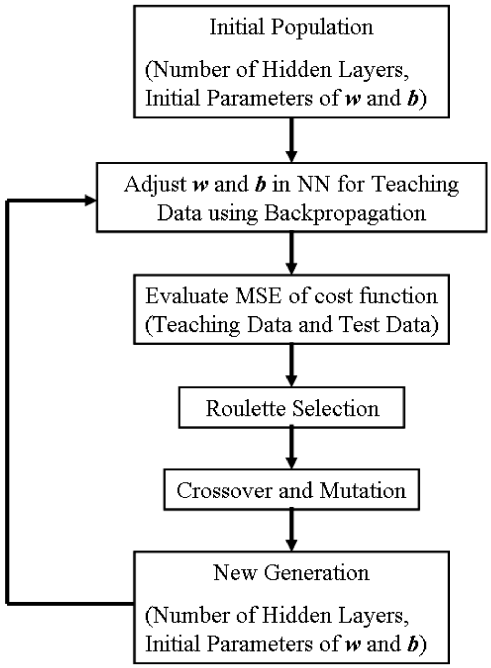

Fig. 3 GA optimization of NN.

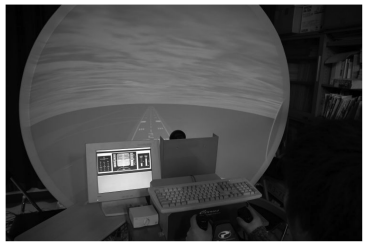

Fig. 4 Flight simulator.

Table 1 Simulated flight conditions

Weight	240,000 lb
Initial altitude	300 ft
Initial path angle	−3 deg
Initial velocity	239.4 ft/s
Initial distance from the runway front edge	5224 ft

calculated. The roulette selection method is used to select a few parent strings. This is a stochastic selection method, in which the lower the cost function of a gene, the greater the probability it will be selected. Mutation and crossover are introduced to impart probabilistic search characteristics to the GAs. The mutation is to change the binary randomly, to prevent convergence to a local solution. The crossover operator recombines the binary values of 2 genes (parents) into a new gene (child), which will be part of the population in the next iteration (generation). The elite strategy is applied to transfer the best gene to the next generation to prevent excellent solutions from disappearing from the population. The populations are transformed from generation to generation in this loop. More details are presented in [5].

III. Visual Cue Analysis Using PC-Based Simulator

The proposed method is applied to analyze a pilot's longitudinal control process during the final landing phase. A PC-based simulator using mathematical models of midsize jet airliners was used. The simulator was operated by the captain of a Boeing 767 aircraft. Flight data consisting of aircraft positions, pitch angles, and control column and throttle deflections were obtained. The values of visual cues cannot be obtained directly at each sampling time from the flight data, and so they are computed from the runway geometry and the aircraft positions and attitudes.

In the first step, the airline pilot operated the flight simulator using a control column and a throttle lever. The operator observed a parabolic screen that displayed a visual image of the runway and horizon during the final landing phase (as shown in Fig. 4). The flight conditions are summarized in Table 1. Note that only the longitudinal motion was simulated and controlled by the pilot. The visual cues displayed on the screen are represented as shown in Fig. 5, where Y and H are the heights of the horizon and the marker on the runway from the cockpit glare shield, respectively, and θ is the angle of the runway sideline.

In the experiment, the operator was asked to focus on a particular visual cue during the final landing phase. Consequently four cases of flight data were obtained, as follows:

1) *Case normal*: The data were obtained by a normal operation without any restraint.

2) *Case horizon*: The operator intentionally used the horizon as the main visual cue.

3) *Case runway*: The operator intentionally used the angle of the runway side as the main visual cue.

4) *Case marker*: The operator intentionally used the runway marker as the main visual cue.

For each case, one set of flight data for a successful landing was recorded after several trials. Figures 6–9 show the flight paths, pitch angles, control column angles, and throttle positions that were recorded for each case. These results indicate that a smooth landing was achieved in case normal and case marker. On the other hand, in case horizon and case runway, direct landing failed and had to be reattempted for realizing a smooth landing. It is considered that a pilot predominantly uses the horizon and the runway sideline to estimate the pitch angle and the height of the plane; however the

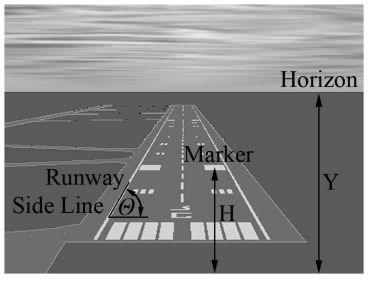

Fig. 5 Visual cues.

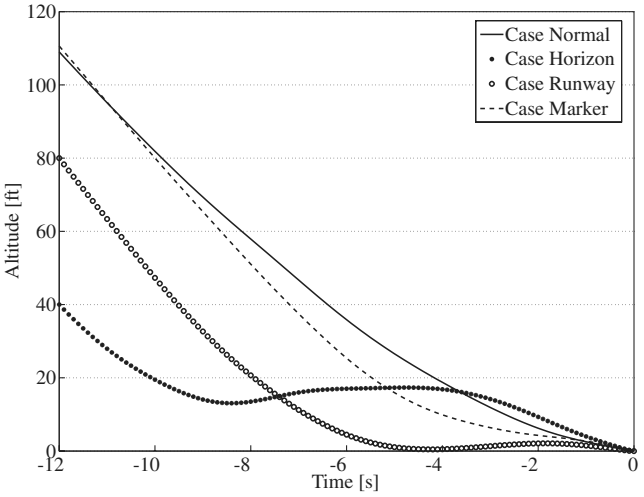

Fig. 6 Recorded flight path for each case.

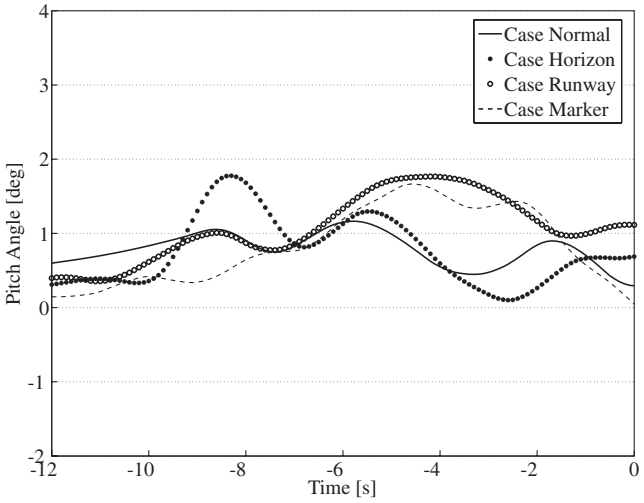

Fig. 7 Recorded pitch angle for each case.

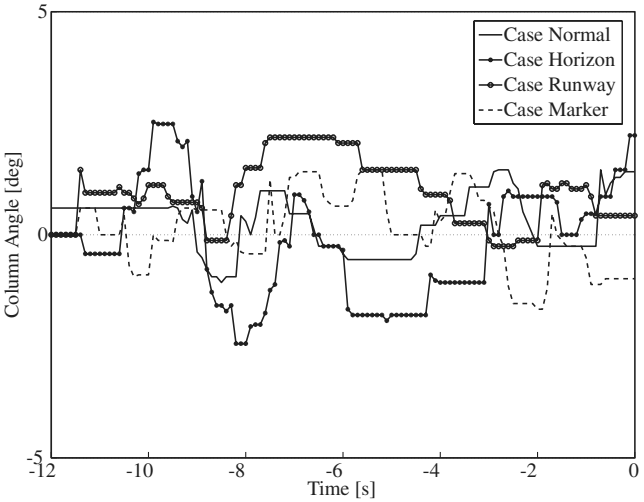

Fig. 8 Recorded column angle for each case.

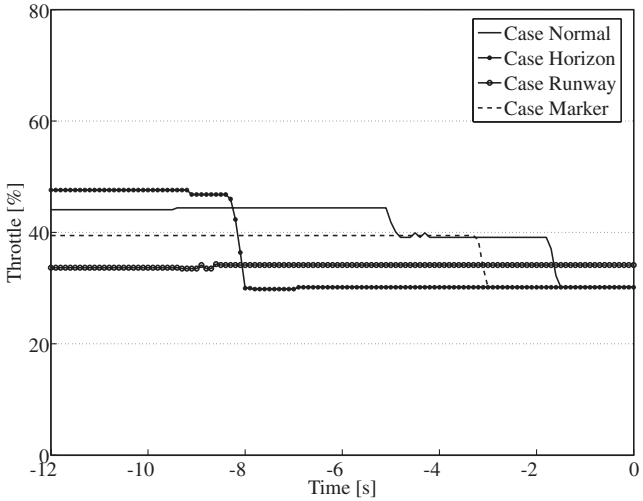

Fig. 9 Recorded throttle position for each case.

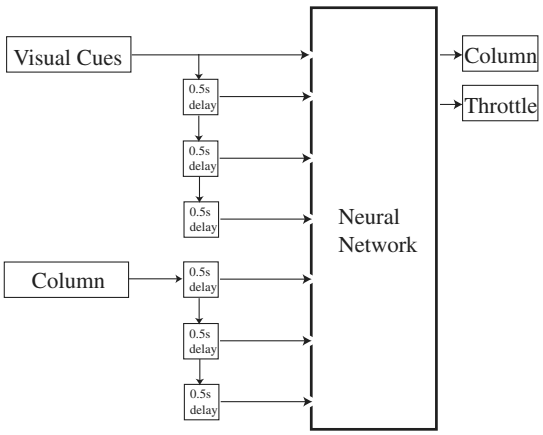

Fig. 10 Inputs and outputs of the network.

intentional focus on these visual cues in case horizon and case runway leads to a nonsmooth landing.

To analyze the landing performance in the four cases, NN models were obtained for each case. Figure 10 illustrates the input and output data of the network. It must be noted that not only the present data but also the time-lagged data were used as the input data of the network, and the time-lagged column deflections are also applied to the NN inputs; this is because memories of earlier visual cues and column positions influence the pilot control inputs at a particular moment. Although the column deflection is not a visual cue, it is treated similarly as a visual cue, and its contribution is also calculated. The

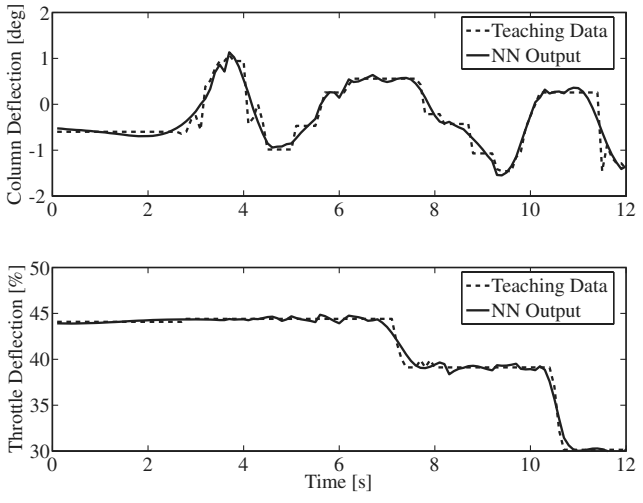

Fig. 11 Teaching data and outputs of neural network (case normal).

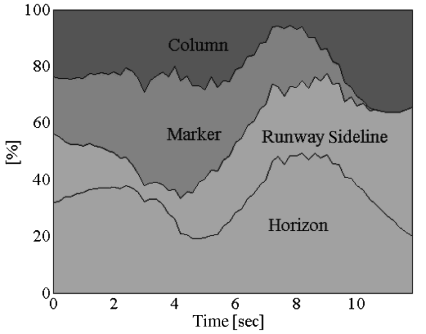

Fig. 12 Contribution ratios (case normal).

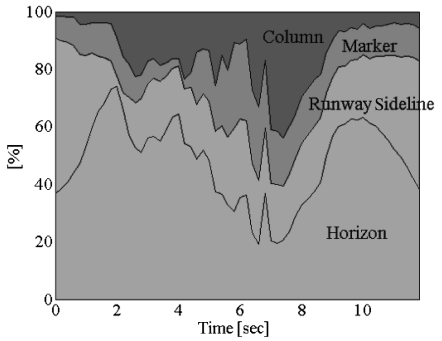

Fig. 13 Contribution ratios (case horizon).

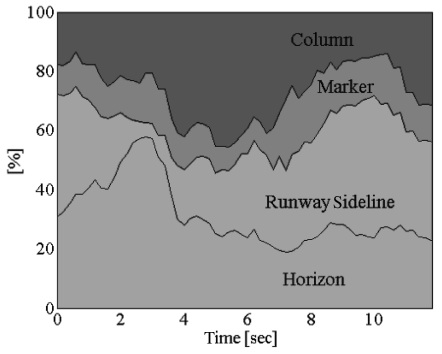

Fig. 14 Contribution ratios (case runway).

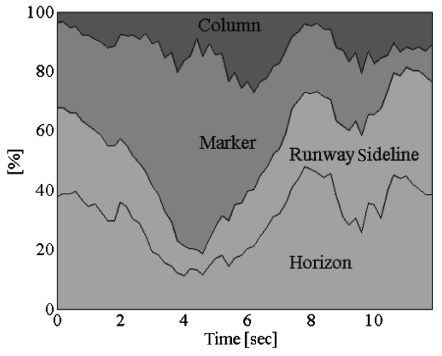

Fig. 15 Contribution ratios (case marker).

sampling rate of data acquisition was 10 Hz, and the time-lagged data were selected as follows: −0.5, −1.0, and −1.5 s.

The outputs of the network are pilot control movements: control column and throttle deflections. The flight data obtained 12 s before touchdown was used to teach the NN. Figure 11 shows a comparison of the recorded deflections of the control column and the throttle with the control data computed by the obtained NN model; there is an excellent agreement between the two results. NN models were obtained for all four cases and were found to exhibit similar agreement.

In the first step, the contribution ratios of the inputs to the column were calculated from Eq. (6). The contribution ratios during each landing case are compared in Figs. 12–15. In case normal, as shown in Fig. 12, the main visual cue shifts sequentially from horizon (0–3 s), marker (3–6 s), horizon (6–9 s), to column and runway sideline (9–12 s). This indicates that the pilot selected the main visual cue in response to each landing phase. Figures 13–15 illustrate the contribution ratios for the special landing cases where the pilot intentionally used a specified visual cue. It can be said that the contribution ratio from the input that is intentionally used as the main visual cue is higher than that in case normal. For example, in case horizon, a high contribution ratio for the horizon is exhibited, as shown in Fig. 13; here, the pilot intentionally used the horizon as the main visual cue. This implies that the restraint provided to the operator can appropriately affect the analysis results. Therefore it is considered that the obtained NN models properly represent the landing characteristics for each case.

In the second step, automated landing simulations were carried out, that is, the obtained NN models were used as automatic controllers in the flight simulations to clarify the characteristics of each network. Figures 16–19 show the simulation results for each case. The initial flight condition is described based on the trimmed condition along the glide slope, except that the initial altitude is distributed over a range of 20 ft around the glide slope. It is noted that on the horizontal axis, "X = 0" indicates the front edge of the runway. In addition, Fig. 20 summarizes the average values and the standard deviations (SD) of the sink rate (ft/min), the pitch angle (degree) at touchdown, and the distance from the front edge of the runway to the touchdown point. This calculation is based on the Monte Carlo simulation, which randomly distributes the initial altitudes. One hundred landings were carried out for each simulation of the four cases. The characteristics of each case can be summarized as follows:

1) *Case normal*: Figure 20 indicates that case normal is consistently capable of a successful landing with a low sink rate and a safe pitch angle. The dispersions of all the parameters are very low, which implies that case normal enables stable landing. Figure 16 also shows this result, that is, the time histories of pitch angle show an appropriate maneuver at the flare phase to decrease the sink rate.

2) *Case horizon*: As shown in Fig. 20, in case horizon, the pitch angles converge to small values because the horizon information can be used to obtain the pitch angle information. However the touchdown points are distributed over a wide range and the sink rates are relatively high. This is because horizon information cannot be used to determine altitude information. Figure 17 shows that the NN in case horizon could not determine the timing of the flare maneuver and attempted the landing again. This is recognized in the original recorded data of case horizon in Fig. 6.

3) *Case runway*: Figure 20 indicates that case runway is almost perfectly capable of a successful landing, particularly with the low standard deviations of all the parameters. Although the original recorded data of case runway in Fig. 6 could not be used to accurately determine the landing timing and the landing had to be reattempted, the simulation results indicate a stable landing. This is because the initial conditions are different from the recorded results. It is considered that the runway sideline can be used to determine the altitude. Therefore it is difficult to control the pitch angle in case runway, as shown in Fig. 18, where the flare control is insufficient. This is because both the sink rate and the pitch angle are higher than those in case normal.

4) *Case marker*: Although the original recorded data of case marker in Fig. 6 indicated a smooth landing, the simulation results

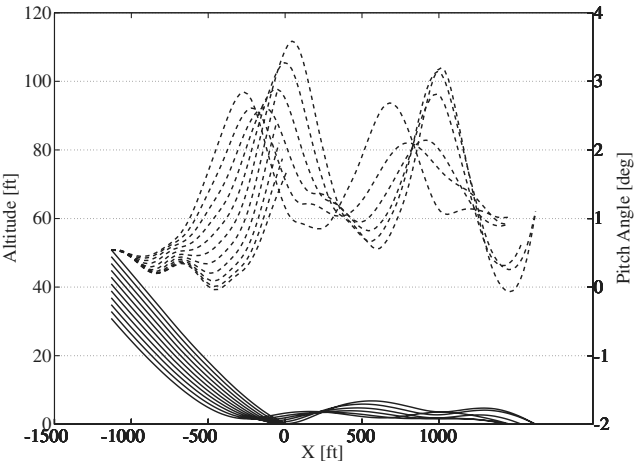

Fig. 17 Neural network controlled simulation results (case horizon).

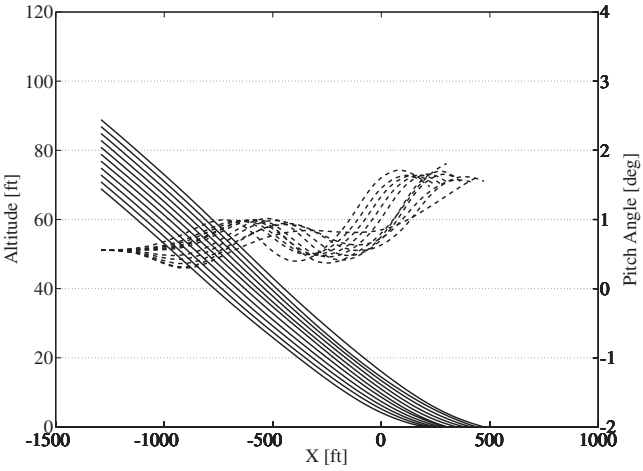

Fig. 18 Neural network controlled simulation results (case runway).

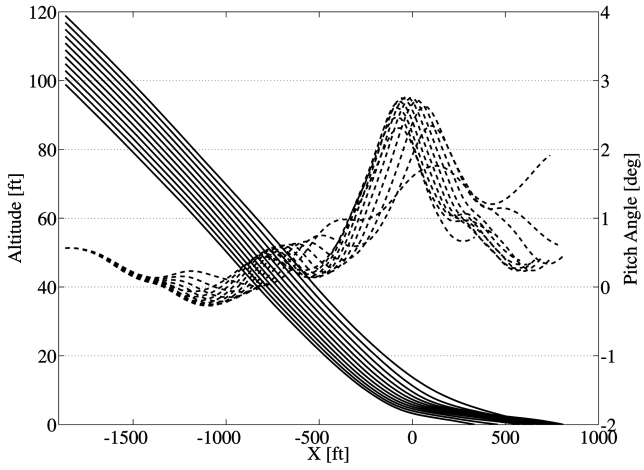

Fig. 16 Neural network controlled simulation results (case normal).

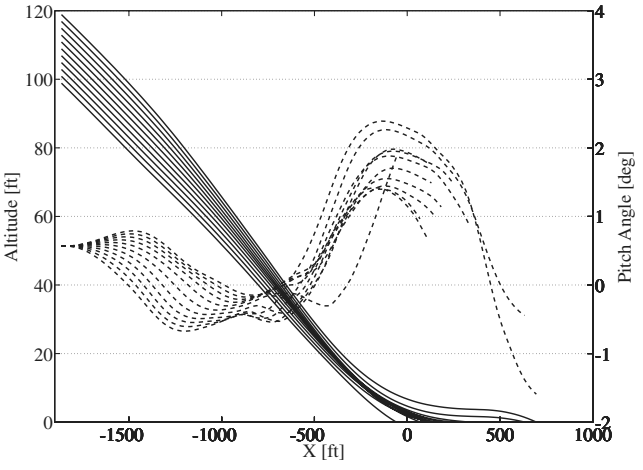

Fig. 19 Neural network controlled simulation results (case marker).

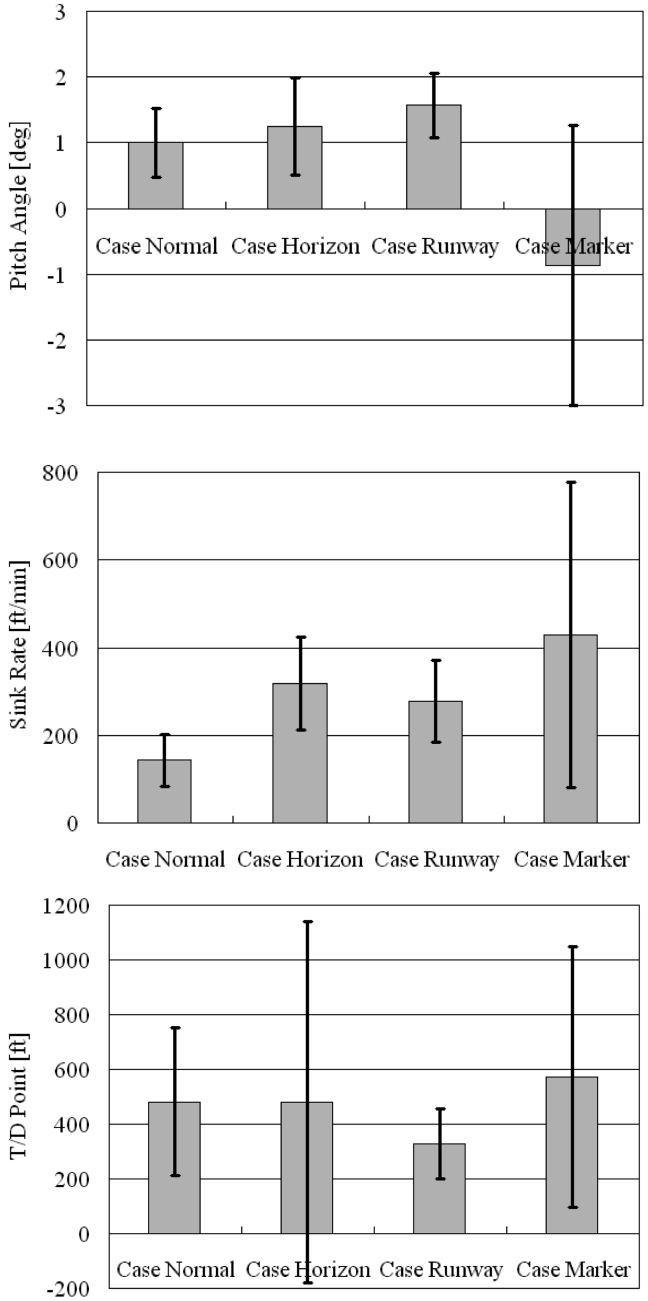

Fig. 20 Results of Monte Carlo landing simulations.

show that in case marker, the pitch angle and the sink rate could not be controlled. This is because it is difficult to use the marker to recognize pitch information. The simulation results reveal that the NN model of case marker does not have sufficient landing capabilities.

The simulation results are summarized again in Table 2, where the success ratios are evaluated from the Monte Carlo simulation for each case. The assumed criteria are as follows: 1) the sink rate at touchdown is less than 400 ft/ min, 2) the pitch angle at touchdown is greater than 0 deg, and 3) the touchdown point is on the runway ($X > 0$ for the landing). Only case normal satisfies all the criteria; thus, it is confirmed that the appropriate shifting of the main visual cue as used in case normal is important for a stable and robust landing maneuver.

IV. Conclusions

Neural network modeling has been applied to analyze the cognitive process and control maneuvers of a human pilot by using the recorded flight data from a flight simulator. This paper investigates the role of visual cues such as the horizon, runway side lines, and runway marker during the final landing phase for a midsize jet airliner. Different flight data were obtained by using a PC-based flight simulator when a pilot was asked to intentionally concentrate on a specified visual cue. The obtained contribution ratio of each visual cue to the pilot column movement indicates that specified visual cues have a higher contribution ratio than that obtained from the normal operation. This implies that the obtained NN models can appropriately express the pilot's intentions. The Monte Carlo flight simulations using the obtained NN models as automatic controllers were performed to determine the role of each visual cue. The evaluation of the terminal sink rate/pitch angle and the touchdown point for each simulation qualitatively clarified the role of each visual cue. The horizon is useful to estimate the pitch attitude and should be focused at the flare maneuver. However because it is difficult to recognize the height from the horizon, the runway sideline should be used as an important visual cue for an accurate landing maneuver. Although the runway marker indicates the landing point, it is very difficult to control an aircraft attitude from the runway marker. The Monte Carlo landing simulations imply these results. These results also agree with the pilot textbook and pilot's comment. Of course, close attention to the specific visual cue resulted in the unsuccessful landing, and the equal attention to all visual cues are not also recommended. It is confirmed that an appropriate choice of visual cues is important for a smooth and robust landing maneuver.

References

[1] Hess, R. A., and Beckman, A. A., "An Engineering Approach to Determining Visual Information Requirements for Flight Control Tasks," *IEEE Transactions on Systems, Man, and Cybernetics*, Vol. SMC-14, No. 2, 1984, pp. 286–298.

[2] Schmidt, D. K., and Silk, A. B., "Modeling Human Perception and Estimation of Kinematic Responses During Aircraft Landing," AIAA Paper 88-4186-CP, 1988.

[3] Kuriki, Y., Suzuki, S., Uemura, T., and Kitaki, Y., "Research on State Estimation of Pilot in Landing Aircraft," *Journal of the Japan Society for Aeronautical and Space Sciences*, Vol. 49, No. 571, 2001, pp. 246–254 (in Japanese).

[4] Kageyama, I., and Arai, A., "Research on Driver's Information Process at Accident-Prone Area," *Proceedings of the 7th Transportation and Logistics Conference*, Japanese Society of Mechanical Engineers, Tokyo, 2003, pp. 227–230 (in Japanese).

[5] Suzuki, S., Sakamoto, Y., Sanematsu, Y., and Takahara, H., "Analysis of Human Pilot Control Inputs Using Neural Network," *Journal of Aircraft*, Vol. 43, No. 3, 2006, pp. 793–796.

[6] Arbib, M. A., *Brains, Machines and Mathematics*, 2nd ed., Springer–Verlag, New York, 1987.

[7] Takahara, H., Kondo, T., and Suzuki, S., "Study of Landing Technique During Visual Approach," *Proceedings of the 24th International Council of the Aeronautical Sciences Congress*, International Council of the Aeronautical Sciences, Stockholm, 2004; International Council of the Aeronautical Sciences Paper ICAS2004-7.11.2.

[8] Holland, J., *Adaptation and Natural and Artificial System*, Univ. of Michigan Press, Ann Arbor, MI, 1975.

Table 2 Landing simulation results

	Sink rate, avg/SD	Pitch angle, avg/SD	T/D point, avg/SD	All satisfied
Normal	100% (143/59)	100% (1.00/0.53)	100% (482/270)	100%
Horizon	71% (318/107)	98% (1.24/0.74)	75% (482/660)	65%
Runway	92% (277/93)	95% (1.57/0.49)	100% (327/128)	92%
Marker	69% (429/348)	35% (−0.87/2.13)	89% (572/477)	34%